Soft Motion of Dielectric Driven Balloon Actuator

Nishira, Yoshinobu
Department of Aeronautics and Astronautics, Kyushu University

Ito, Kosei
Department of Aeronautics and Astronautics, Graduate, Kyushu University

Tsumori, Fujio
Department of Aeronautics and Astronautics, Kyushu University

https://hdl.handle.net/2324/7178656

出版情報：Journal of Photopolymer Science and Technology. 36 (3), pp.191-195, 2023-06-15. フォトポリマー学会
バージョン：

Journal of Photopolymer Science and Technology
Volume 36, Number 3 (2023) 191－195 ©2023SPST

Soft Motion of Dielectric Driven Balloon Actuator

Yoshinobu Nishira, Kosei Ito, and Fujio Tsumori*

Department of Aeronautics and Astronautics, Kyushu University,
744 Motooka, Nishi-ku, Fukuoka 819-0395, Japan
**tsumori @aero.kyushu-u.ac.jp*

This study presents the development of a balloon-type dielectric elastomer actuator (DEA) that utilizes the Maxwell stress generated by applying voltage between electrodes. DEAs have been recognized for their superior responsiveness, durability, and energy efficiency, making them a promising candidate for applications such as artificial muscles. We fabricated two types of DEA using a latex balloon as the elastic material and carbon grease as the electrode to generate inflating and squashed deformations. We conducted experiments to measure and analyze the two types of deformation while varying the size or inner pressure of the balloon and the voltage magnitude. We found that the voltage magnitude affected the magnitude of the deformation in the actuator with inflating deformation, but not in the actuator with squashed deformation. Additionally, we estimated the applied Maxwell stress in the actuator. The developed actuators were capable of producing movements that imitate the behavior of organisms, such as the pufferfish.
Key words: Soft actuator, DEA, Balloon, Maxwell stress

1. Introduction

Soft actuators have gained significant attention due to their flexibility and ability to generate a variety of movements such as crawling [1, 2], jumping [1, 3], grasping [3, 4], and bending [5]. Compared to conventional rigid actuators, soft actuators can move delicately, resulting in low noise levels and high adaptability to the surrounding environment. With their lightweight and soft bodies, soft actuators are expected to find applications in the medical and aerospace fields. They can be driven by various inputs, including pneumatic [2, 4, 5], magnetic [6-15], thermal [16, 17], and electrical [18-31] methods. In this study, we focus on electrically-driven soft actuators and have developed dielectric elastomer actuators (DEAs) due to their superior responsibility, durability, and energy efficiency [29].

DEAs are typically composed of a thin film possessing dielectric properties, sandwiched between two deformable electrodes as shown in Fig. 1. When a high voltage is applied between the electrodes, the resulting attractive force, known as the Maxwell stress, causes the dielectric film to deform elastically, becoming thinner while extending in the planar direction.

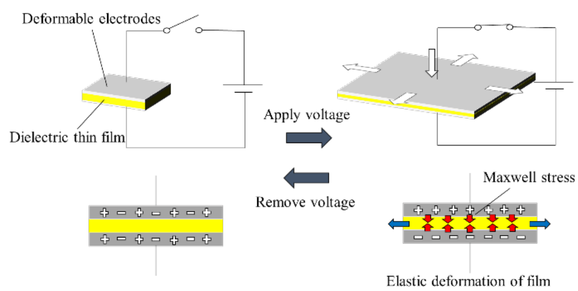

Fig. 1. Principle of DEA operation

In this study, we experimentally analyze the deformation of a balloon-type DEA. While previous studies have developed DEAs generating bending [25] and stretching [26] deformations, our actuator produces inflating and squashed deformations using natural rubber latex balloons as the material. The actuators are fabricated by placing an electrode inside a latex balloon and subsequently inflating it. We measure the resulting deformations when a high voltage is applied, and estimate the applied Maxwell stress to the actuator based on the results.

2. Developed Balloon-type DEA

This section describes the materials and methods used to fabricate and actuate the balloon type DEA.

Received April 9, 2023
Accepted April 9, 2023

The actuator was fabricated using a latex balloon made from natural rubber (Pioneer Balloon) and antistatic grease (Sunhayato, GE-L201) as the electrode. High voltages were applied to the actuators using an AC/DC high voltage generator (Advanced Energy Industries, TREK 610E).

Two types of actuators were fabricated in this study: inflated and squashed. To fabricate the actuator with inflating deformation, carbon grease was applied to the inside and outside of a latex balloon that was then inflated as shown in Fig. 2. For the actuator with squashed deformation, the carbon grease was coated only inside the balloon, and the balloon was placed on a metal substrate and connected to a high voltage generator. Schematic setups of the both actuators are shown in Figs. 3 and 4, respectively. In both cases, the Maxwell stress between the carbon grease inside and outside the balloon resulted in the desired deformation.

To measure the deformation, we varied the size

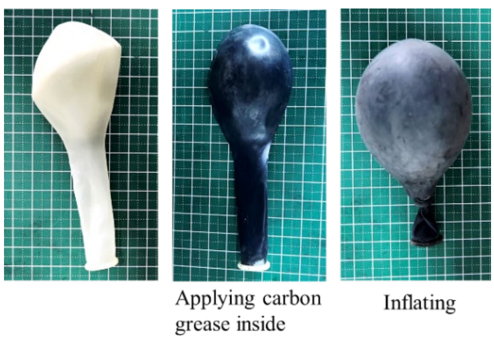

Fig. 2. Actuator creation process

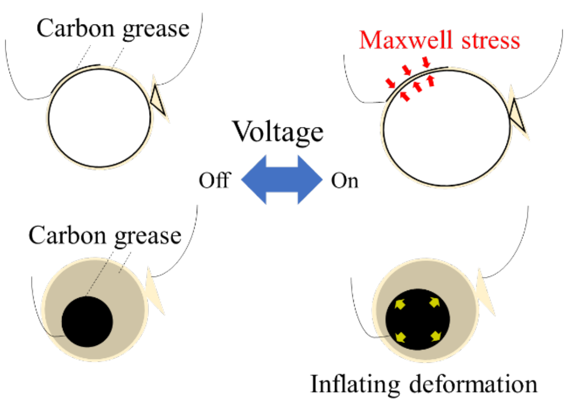

Fig. 3. Structure of the actuator with inflating deformation

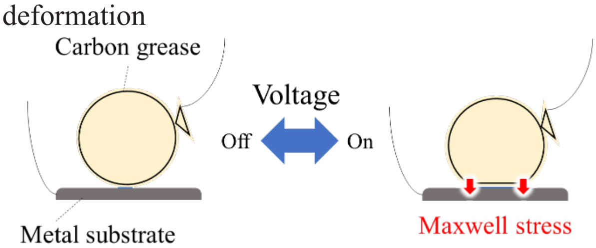

Fig. 4. Structure of the actuator with squashed deformation

(or inner pressure) of the balloon and the magnitude of the voltage applied to the actuator. The measurements and analyses of the deformation were performed using a video. The video images were processed by an image processing software (ImageJ) and a markerless pose estimation software based on a machine learning system with deep neural networks (DeepLabCut). The Maxwell stress applied to the actuator was estimated based on the deformation results and discussed in the following section.

3. Experiment

3.1. Actuator with inflating deformation

The actuator with inflating deformation was operated at different voltages while varying the diameter of the balloons. The actuated balloons are shown in Figure 5. The voltage range applied was from 0 to 5 kV. Once the voltage was initiated, the carbon grease on the surface of the actuator expanded in area, resulting in a noticeable deformation that increased slightly as the voltage was increased. The relationship between the deformation and the voltage is shown in Fig. 6. As the voltage increased, the Maxwell stress also increased, resulting in a corresponding increase in the deformation. At high voltages, the actuator sometimes experienced a dielectric breakdown as the short diameter decreased. This breakdown could be attributed to the Maxwell stress further thinning the dielectric film, which was already reduced due

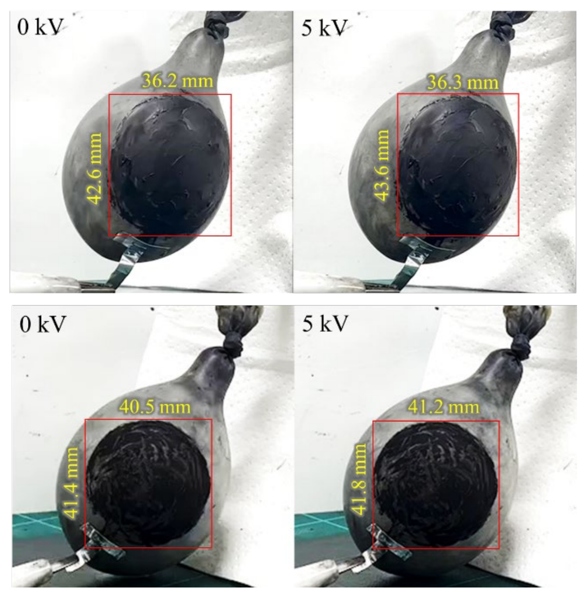

Fig. 5. Deformation of the actuator with inflating deformation. The diameter of the balloon was 50 mm (upper), and 55 mm (lower)

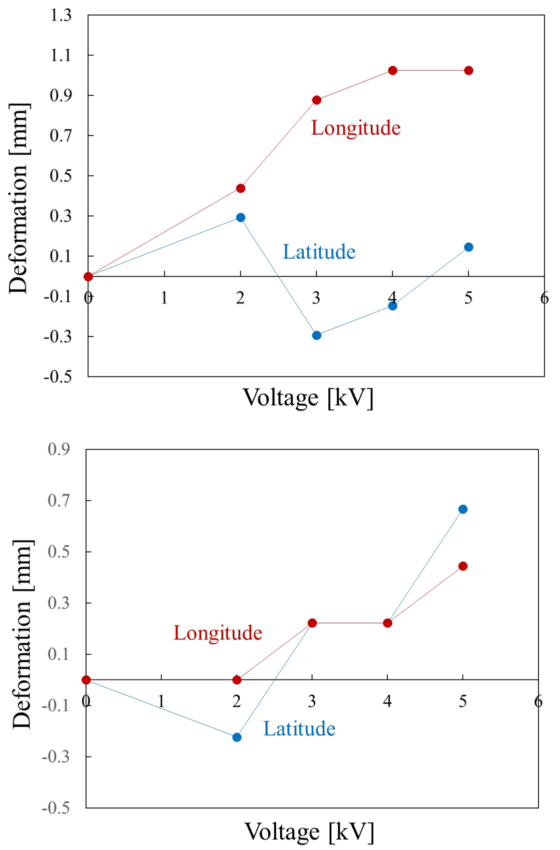

Fig. 6. Deformation of the actuators. The diameter of the balloon was 50 mm (upper), and 55 mm (lower)

to the balloon's enlargement. meter of the balloon increased due to the occurrence of electrical breakdown. This dielectric breakdown can be considered to have been caused by the Maxwell stress further thinning the film thickness, which was reduced by the balloon's enlargement.

3.2. Actuator with squashed deformation

3.2.1. Characteristics of balloons

Prior to performing the experiment of the actuator with squashed deformation, we conducted an experiment to measure the deformation properties of the latex balloons. This experiment involved applying a vertical force to a balloon placed on an electrical balance and measuring the load. The deformation was measured for each internal pressure of the balloon, and the results are shown in Fig. 7. As shown, the deformation decreases as the internal pressure of the balloon increases.

When a vertical load is applied to a balloon, the force F is given by the following equation:

$$F = \frac{\pi D^2}{4} \Delta p \qquad (1)$$

where D is the contact diameter, and Δp is the pressure difference between inside and outside of a balloon. The relationship between the vertical force to a balloon and the contact diameter determined this theoretical equation, and qualitatively similar as the experimental results.

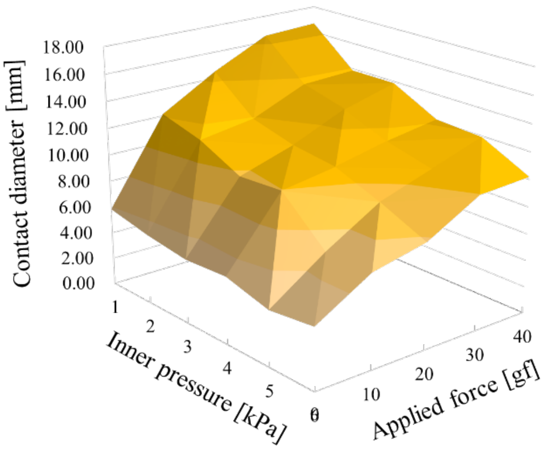

Fig. 7. Change of contact diameter of the balloon on the substrate

3.2.2. Deformation measurement

The results of applying voltages of 0-5 kV while varying the internal pressure of the balloon are shown in Fig. 8. The measured contact diameter between the metal substrate and the balloon for each case is shown in Fig. 9. The deformation was smaller at 1 kV. The deformation would not reach the peak value because the Maxwell stress was too small. For voltages of 2 kV and above, there was little difference in the size of the deformation due to voltage, indicating that the deformation of this actuator was independent of the applied voltage. The reason for the lack of deformation at an internal pressure of 6 kPa would be due to nonlinear deformation of the natural rubber. The rubber would be stiffer just before reaching an internal pressure of 6 kPa.

The contact diameter results obtained and the perpendicular force applied when a voltage is applied were estimated using equation (1). Figure 10 shows the case of the applied voltage of 5 kV. The vertical force was decreasing where the internal pressure of the balloon exceeds 4 kV. This is considered to be due to the nonlinearity of rubber elasticity.

4. Conclusion

We produced balloon type DEA that cause inflating and squashed deformation. We created two types of actuators that differed in the inner pressure

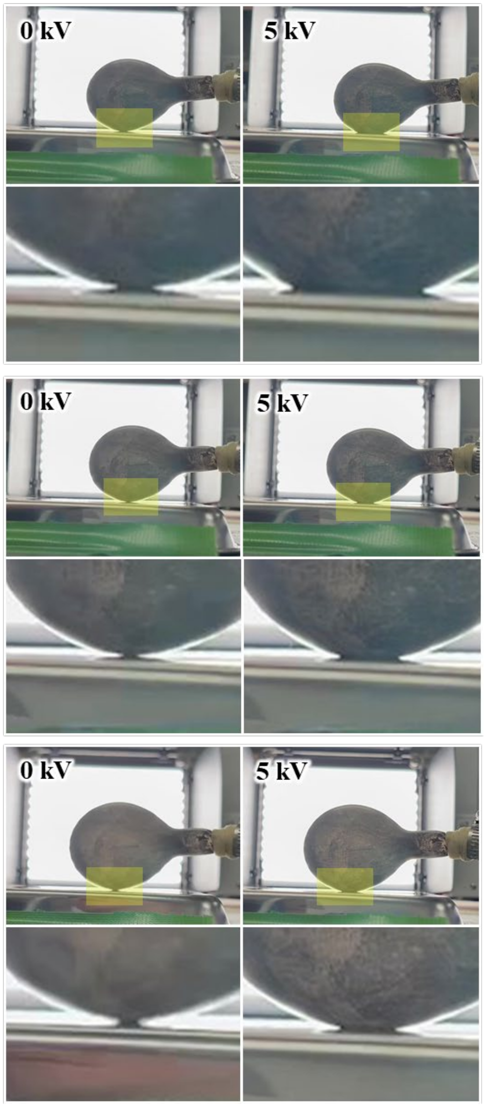

Fig. 8. Deformation of the actuator with squashed deformation. Inner pressure 1 kPa (upper), 3 kPa (center), and 5 kPa (lower).

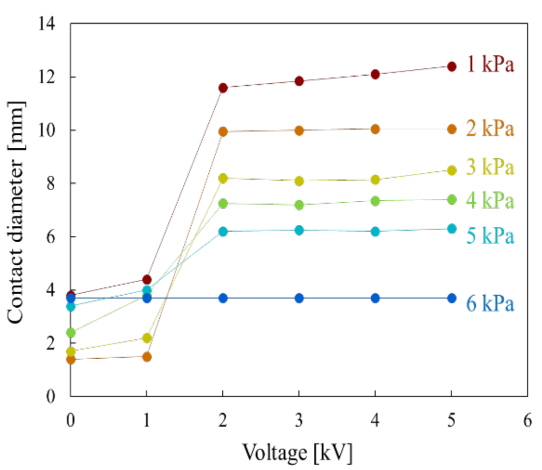

Fig. 9. The result of applying voltage to the actuator with squashed deformation

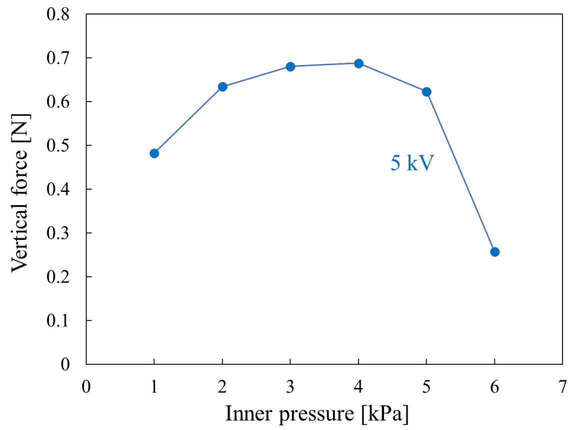

Fig. 10. Maxwell stress estimates

of the balloon and applied voltage, and we measured the deformation for each type. In the actuator with inflating deformations, we observed a slight variation in the amount of deformation with increasing voltage. For the actuator with squashed deformation, we noted a negligible difference in deformation magnitude despite applying varying voltage levels. Also, the value of Maxwell stress could be estimated by comparing the deformation when a vertical load was applied with that when a voltage was applied. These actuators could produce movements that mimic organisms such as pufferfish.

Acknowledgements

This work was supported by MEXT KAKENHI Grant Numbers JP22H05685 and JP23H04319.

References

1. W. Huang, W. Shang, Y. Huang, H. Long, and X. Wu, *IEEE Robot. Autom. Lett.*, **7** (2022) 9287.
2. R. F. Shepherd, F. Ilievski, W. Choi, S. A. Morin, A. A. Stokes, A. D. Mazzeo, X. Chen, M. Wang, and G. M. Whitesides, *Proc. Natl. Acad. Sci. U S A*, **108** (2011) 20400.
3. C. Tawk, R. Mutlu, and G. Alici, *Front. Robot. AI*, **8** (2022) 799230.
4. R. Deimel and O. Brock, *IEEE Int. Conf. Robot. Autom.*, (2013) 2047.
5. H. M. Elmoughni, A. F. Yilmaz, K. Ozlem, F. Khalilbayli, L. Cappello, A. T. Atalay, G. Ince, and O. Atalay, *Actuators*, **10** (2021) 3390.
6. W. Zhang, Y. D. J. Zhao, T. Zhang, X, Zhang, W. Song, L. Wang, and T. Li, *Small*, (2023)
7. Z. Wu, Q. Wang, J. Huang, Y. Yue, D. Chen, Y. Shi, and B. Su, *Compos. Sci. Technol.*, **217** (2022) 109129.
8. F. Tsumori, A. Saijou, T. Osada, and H. Miura, *Jpn J Appl Phys*, **54** (2015) 6.

9. H. Shinoda, S. Azukizawa, K. Maeda, and F. Tsumori, *J. Electrochem. Soc.*, **166** (2019) B3235.
10. F. Tsumori, R. Marume, A. Saijou, K. Kudo, T. Osada, and H. Miura, *Jpn. J. Appl. Phys.*, **55** (2016) 06GP19.
11. R. Marume, F. Tsumori, K. Kudo, T. Osada, and K. Shinagawa, *Jpn. J. Appl. Phys.,* **56** (2017) 06GN15.
12. S. Azukizawa, H. Shinoda, K. Tokumaru, and F. Tsumori, *J. Photopolym. Sci. Technol.*, **31** (2018) 139.
13. F. Tsumori, N. Miyano, and H. Kotera, *J. Jpn. Soc. Powder Powder Metal.*, **56** (2009) 133.
14. F. Tsumori, H. Kawanishi, K. Kudo, T. Osada, and H. Miura, *Jpn. J. Appl. Phys.*, **55** (2016) 06GP18.
15. F. Tsumori and J. Brunne, in *Proceedings of the IEEE International Conference on Micro Electro Mechanical Systems (MEMS)* (2011).
16. T. H. Ware, M. E. McConney, J. J. Wie, V. P. Tondiglia, and T. J. White, "Voxelated liquid crystal elastomers," *Science*, **347** (2015) 982.
17. Y. Yang, Z. Pei, Z. Li, Y. Wei, and Y. Ji, *J. Am. Chem. Soc.*, **38** (2016) 2118.
18. T. G. La and G. K. Lau, *Appl. Phys. Lett.*, **102** (2013) 192905.
19. J. Ashby, S. Rosset, E. F. M. Henke, and I. A. Anderson, *Front. Robot. AI*, **8** (2022) 792831.
20. P. White, S. Latscha, and M. Yim, *Actuators*, **3** (2014) 245.
21. Y. Liu, B. Liu, T. Yin, Y. Xiang, H. Zhou, and S. Qu, *Smart Mater Struct*, **29** (2020) 15008.
22. D. Gonzalez, J. Garcia, and B. Newell, *Sens. Actuator A Phys.*, **297** (2019) 111565.
23. J. Bernat and J. Kołota, *Energies,* **14** (2021) 5633.
24. A. Wiranata, Y. Ishii, N. Hosoya, and S. Maeda, *Adv Eng Mater*, **23** (2021) 2001181.
25. F. A. Mohd Ghazali, C. K. Mah, A. AbuZaiter, P. S. Chee, and M. S. Mohamed Ali, "Soft dielectric elastomer actuator micropump," *Sens. Actuators A Phys.*, **263** (2017) 276.
26. Y. Zhu N. Liu, Z. Chen, H. He, Z. Wang, Z. Gu, Y. Chen, J. Mao, Y. Luo, and Y. He, *ACS Mater. Lett.*, **5** (2023) 704.
27. M. Molberg, Y. Leterrier, C. J. G. Plummer, C. Walder, C. Lowe, D. M. Opris, F. A. Nuesch, S. Bauer, and J. A. E. Manson, *J. Appl. Phys.*, **106** (2009) 054112.
28. R. Pelrine, R. Kornbluh, Q. Pei, and J. Joseph, "High-speed electrically actuated elastomers with strain greater than 100%," *Science*, **287** (2000) 836.
29. N. Koike and T. Hayakawa, *ROBOMECH J.*, **8** (2021) 2055.
30. H. Zhao, A. M. Hussain, M. Duduta, D. M. Vogt, R. J. Wood, and D. R. Clarke, "Compact Dielectric Elastomer Linear Actuators," *Adv. Funct. Mater.*, **28** (2018) 1804328.
31. J. Shintake, V. Cacucciolo, H. Shea, and D. Floreano, *Soft Robot.*, **5** (2018) 46.